Vol. 22, No. 3(2023) Sim2347
Revista Mexicana de Ingeniería Química

# Entropy and Hurst analysis for the determination of two-phase flow time series complexity

# Entropía y análisis de Hurst para la determinación de la complejidad de series temporales de flujo bifásico

A. Marin-Lopez[1]*, H. Puebla[2], J. A. Martínez-Cadena[3], J. Alvarez-Ramirez[1]
[1]*Departamento de Ingeniería de Procesos e Hidráulica. Universidad Autonoma Metropolitana-Iztapalapa. Apartado Postal 55-534, Iztapalapa, CDMX, 09340 México.*
[2]*Departamento de Energía. Universidad Autonoma Metropolitana-Azcapotzalco. Av. San Pablo 180, Col. Reynosa, Azcapotzalco, CDMX, 02200 México.*
[3]*Departamento de Matemáticas. Universidad Autonoma Metropolitana-Iztapalapa. Apartado Postal 55-534, Iztapalapa, CDMX, 09340 México.*
Received: May 25, 2023; Accepted: September 9, 2023

## Abstract
The complexity in time series of two-phase flow is associate with the interaction of gas bubbles and liquid phase, this interaction shows characteristic that depend on different condition such as low rate, physical properties phases, geometry, and tube inclination, etc. This work uses singular value decomposition (SVD) entropy and rescaled range analysis (R/S) to evaluated complexity in voltage signals of four flow patterns. Entropy helps to understand the complexity of each flow pattern, while R/S analysis allows detecting long-range correlations that exist in a time series. Results shows the entropy by SVD and R/S analysis in time series are interesting techniques that can use for the identification of flow patterns with the advantage that are easy to use and implement due to their low computational cost.
*Keywords*: flow-pattern, fractal analysis, entropy, voltage series.

## Resumen
La complejidad en las series temporales de flujo bifásico está asociada con la interacción de las burbujas de gas y la fase líquida, esta interacción muestra características que dependen de diferentes condiciones como las velocidades de flujo, las propiedades físicas de las fases, la geometría y la inclinación del tubo, etc. Este trabajo utiliza la entropía a través de descomposición de valores singulares (SVD) y el análisis de rango reescalado (R/S) para evaluar la complejidad en las señales de tensión de cuatro patrones de flujo. La entropía ayuda a comprender la complejidad de cada patrón de flujo, mientras que el análisis R/S permite detectar las correlaciones de largo alcance que existen en una serie temporal. Los resultados muestran que la entropía por SVD y el análisis R/S en series temporales son técnicas interesantes que pueden utilizarse para la identificación de patrones de flujo con la ventaja de que son fáciles de utilizar e implementar debido a su bajo coste computacional.
*Palabras clave*: flujo bifásico, análisis fractal, entropía, series de voltaje.

* *Corresponding author. E-mail*: marinlopabi@gmail.com
https://doi.org/10.24275/rmiq/Sim2347
*ISSN*:1665-2738, *issn-e*: 2395-8472

# 1 Introduction

In a wide range of industrial process there is the need for flows through pipelines. Some examples are flows in condenser, reactors, heat exchanger, and others. The importance of prediction gas-liquid flow patterns depends on the natural understanding of their interactions. These interactions are manifested in the flow properties, rate flow, diameter, inclination in pipeline, etc. (Firouzi & Hashemabadi, 2009). This is reflected in the design, operation, and handling of fluids in industrial processes. For example, in the oil industry the simultaneous flow of liquid and gas through pipelines is widely present. When gas and liquid flow through a pipeline, various flow patterns can occur, depending on the geometry, pipe size, fluid properties, flow rates and direction, as well as the shape and inclination of the pipeline (Kleinstreuer & Griffith, 2004; Rouhani & Sohal, 1983).

The complexity of two-phase flow patterns is associated with chaotic behavior that is difficult to analyze. When examining time series of biphasic flows, we wish to determine their complexity according to the definition given by Kolmogorov complexity theory, which defines the complexity of a finite object in terms of the smallest computer program that can reproduce that object. In a time series, it is required that it contain the minimum information necessary to describe a process, that is, that there is no redundant information in the data. In a biphasic flow that has one continuous phase and the other dispersed phase. The dispersed phase can be in the form of gas bubbles (gas) or particles (solid or liquid) of different sizes and shapes. The geometric distribution of phases, known as flow topology, is an important characteristic of two-phase flows because it influences the interactions between phases where mass, momentum, and energy can be exchanged. Thus, the complexity in this process is the result of the intermingled effects of many factors that intervene and enhance each other.

The detailed description of two-phase flow in pipes is made difficult by the existence of an interface between the two phases. For a gas-liquid flow, depending on the flow velocities, physical properties of the phases, pipe geometry and inclination, there is an interface which comes in a wide variety of forms (Aguilar *et al*., 2014). According to the shape of this interface, flow patterns have been characterized in a two-phase system. The most observed flow patterns in the flow of gas-liquid mixtures in horizontal pipes are stratified flow, bubbly flow, annular flow, and slug flow. For downward flow in vertical and inclined pipes, annular and stratified flow predominate (Hernandez, 2008).

Different methods have been studied to identify the flow patterns, of which the following are highlighted: a) visualization and experimental methods. (Kleinstreuer & Griffith, 2004; Rouhani & Sohal, 1983; Cheng *et al*., 2008). b) flow maps obtained from experimental results and theoretical models (Cheng *et al*., 2008; O'Donovan & Grimes, 2020, Wu *et al*., 2017), c) time series analysis based on conventional statistical methods, d) neural networks and e) time series analysis based on unconventional methods, such as chaos theory. These methods aim to discriminate flow patterns based on the information hidden in the fluctuations of a variable (Moguel *et al*., 2021).

Serizawa *et al*. (2002) performed adiabatic flow experiments with vapor-water and air-water flows in microchannels where they obtained that the flow patterns were affected by the surface roughness, as a result they presented a flow pattern map based on experimental observations. In turn, Wu *et al*. (2017) studied the critical factors of pipe geometry; diameters, deviation from vertical, fluid properties and flow conditions that affect the transition from one flow pattern to another.

Recently, work has been published on the specific modeling of the various flow patterns. In general, these models work well with the data sets used in their development. However, few papers have shown a real data set. This may be because direct observation and identification of flow regimes in industrial plant pipelines is difficult, as generally industrial fluids flow in steel pipes and often at high pressures and/or temperatures, which affects the availability of reliable experimental data over a wide range of conditions (Xue *et al*., 2014).

Despite advances in the field of flow pattern identification and analysis, most research has focused on flow in horizontal (or near-horizontal) pipes, which behave differently from vertical flow, where gravity affects the flow. Therefore, the analysis of flow patterns in inclined pipes remains a challenge due to the complexity of phase interactions in two-phase flow (Cheng *et al*., 2008).

Singular value decomposition has been applied to signal processing problems (Abdi, 2007) and recovery information (Shen *et al*., 2020), where the relevance of obtaining correlations in data series lies in the identification of patterns involved in the dynamics of complex processes. Therefore, this paper proposes the use of singular value decomposition (SVD) entropy (Caraiani, 2014) as a suitable framework for the analysis of time series, specifically for the study of the complexity of two-phase flow patterns. SVD-based entropy provides information on the nonlinear structures present in signals of different flow patterns and at different time scales. In addition, in order to know the long-range dependence of a time series, the rescaled range ($R/S$) analysis is

used, which will be explained below, and will be used to determine the Hurst coefficient ($H$). The latter is related to the autocorrelation of the time series. The value of the Hurst coefficient will be in the interval [0,1] and depending on the value that the coefficient takes in the interval, it is possible to determine some characteristics of the process to which said coefficient corresponds. Recognizing the importance of integrating available experimental data, two-phase downward flow data from a stress-time series representing the liquid-gas fraction in a pipe cross section has been used.

## 2 Conceptual framework and methodology

### 2.1 Singular Value Decomposition Entropy

Singular value decomposition entropy is used as a measure of complexity of a time series. The geometrical SVD generates linear transformations, which give an idea of the complexity of a matrix.

Given a time series $\{X(t_i)\}$ obtained as a sequence of real numbers of length $n$, $X(t_i)$ is the given value in time.

$$X(t_i,n) = \{X(t_i), X(t_i+1), \ldots, X(t_i+n-1)\} \quad (1)$$

The following matrix of delayed signals is constructed where the rows are formed by the n delayed subsequences:

$$M = \begin{bmatrix} X(t_i:n) \\ X(t_{i+1}:n) \\ \vdots \\ X(t_{i+n-1}:n) \end{bmatrix} \quad (2)$$

The matrix is correlated if there is a relationship between its row vectors, which indicates that the greatest amount of information is concentrated in a subspace of reduced dimension. On the contrary, the absence of correlations implies that the reduction of dimension leads to loss of information. This means that all row vectors in the matrix without correlations contain the same amount of information and, therefore, no vector can be neglected without suffering a deterioration in the reconstruction capacity of the process.

To analyze the time series of the flow patterns described above, singular value decomposition is proposed as a suitable approach to address the question of whether the matrix $M$ is correlated or not. SVD is a factorization of a matrix into the product of three matrices, for the matrix given by Eq. (2), SVD leads to the factorization of the form:

$$M(t_i;n) = U(t_i;n)\sum(t_i;n)V^T(t_i;n) \quad (3)$$

$U(t_i;n)$ and $V^T(t_i;n)$ are unitary orthogonal matrices ($V^T = V^{-1}$) and $\sum(t_i;n)$ is a diagonal matrix ($n \times n$) formed by the singular values of the matrix of delayed signals. These values are obtained by finding the square root of the non-zero eigenvalues of $MM^T$. Thus, $\sigma_i = \sqrt{\lambda_i}$ corresponds to the i-th singular value of $M(t_i;n)$ which are ordered in decreasing order. So, the first value contains the most information in the system, $\sigma_1 \geq \sigma_2 \geq \cdots \geq \sigma_n$. The columns of $U(t_i;n)$ are the singular vectors on the left side and the columns of $V^T(t_i;n)$ are the singular vectors on the right (Wall *et al*., 2003).

Geometrically the SVD produces a change of coordinates through rotations ($U(t_i;n)V^T(t_i;n)$) and deformation $\sum(t_i;n)$. As an example, is the transformation that the unit circle undergoes after the SVD, $V^T(t_i;n)$ produces the rotation of the sphere, $\sum(t_i;n)$ generates a deformation to an ellipse where the first singular values are the semi-axes and finally, $U(t_i;n)$ produces a rotation of the ellipse. The singular values of the matrix $M(t_i;n)$ reflect the correlation information of the time series $X(t_i)$ for a time horizon of $n$ discrete times.

We can construct a complexity measure with the entropy, using the singular values of the matrix $M(t_i;n)$ following Sabatini (2000). The original idea of entropy dates back to Shannon (1948) and is considered as a statistical measure of randomness and amount of information; the more information there is the less entropy (Rao *et al*., 2004). This is calculated from the distribution of the singular values of the matrix $M(t_i;n)$. First, the singular values are normalized as follows (Caraiani, 2014):

$$\sigma_i(t_i;n) = \frac{\sigma_i(t_i;n)}{\sum_{i=1}^{n}\sigma_i(t_i;n)} \quad (4)$$

Then, the entropy depends on the time scale n. One would like to compare the entropy over a range of n time scales. A normalized entropy is calculated by noting that the maximum entropy for a given time scale is $\ln(n)$. In such a case, all singular values are equal to $1/n$, reflecting that the information is likely to travel without a preferred direction. So, the normalized entropy is given by (Alvarez-Ramirez & Rodriguez, 2021):

$$S_X(t_i;n) = -\frac{1}{\ln(n)}\sum_{i=1}^{n}\sigma_i(t_i;n)\ln(\sigma_i(t_i;n)) \quad (5)$$

For an uncorrelated process (e.g., white noise), $\sigma_i(t_i;n) = 1/n$, $i = 1,\ldots,n$ such that $S_X(t_i;n) = 1$. On the contrary, a matrix where correlations exist one should have that $S_X(t_i;n) < 1$.

### 2.2 Discrete Fourier Transform

In this way, a tool used in the identification of hidden patterns in time series is the discrete Fourier

transform which transforms a function from the time domain to the frequency domain, without altering the information content (Wang, 1984). The discrete Fourier transform of a sequence of N complex numbers $x_0,\ldots,x_{N-1}$ from the time domain to $X_0,\ldots,X_{N-1}$ in the frequency domain is defined as follows:

$$X[k] = \sum_{n=0}^{N-1} x_n e^{-\frac{2\pi i}{N}kn} \tag{6}$$

where $i$ is the imaginary unit and $e^{-\frac{2\pi i}{N}kn}$ represents the $N$-th root of the unit for each $k = 0,\ldots,N-1$. The inverse discrete Fourier transform (IDFT) is given by:

$$x[n] = \frac{1}{N}\sum_{k=0}^{N-1} X_k e^{\frac{2\pi i}{N}kn} \tag{7}$$

for $n = 0,\ldots,N-1$. The complex numbers of $X$ represent the amplitude and phase of different sinusoidal components of the input signal $x$. If we represent $X$ in polar form, we get a sinusoid of amplitude and phase from the modulus and argument of $X$. The magnitude is represented mathematically as follows:

$$M = |X| = \sqrt{Re(X)^2 + Im(X)^2} \tag{8}$$

The phase is obtained from the argument of $X$ as follows:

$$\theta = arg(X) = atan2(Im(X), Re(X)) \tag{9}$$

The Discrete Fourier Transform is used in signal processing by producing a decomposition of the signal into components of different frequencies. In this way, it is possible to obtain relevant information that is not evident in the time domain. The technique is also extended to 2D image processing where it is used to enhance, define or extract information from a digital image.

### 2.3 *Hurts exponent and Rescaled range analysis (R/S)*

Rescaled range analysis (R/S) is a statistical tool used for the analysis of time series dynamics and to determine the presence or absence of long-range dependence in a process (Hurst, 1951). The rescaled range analysis proposed by Hurst was fundamental for the study and characterization of complex time series, such as in the field of financial market (Alvarez-Ramirez *et al*., 2008), price dynamics of high value products (Alvarez-Ramirez *et al*., 2002), climatological series (Meraz *et al*., 2015), among others.

For univariate time series, rescaled rank analysis (R/S analysis) is carried out as follows. The data is center, i.e., the mean is subtracted from the time series, subsequently the run through the mean-adjusted series is performed. In other words, the accumulated deviations are obtained.

$$Z(t_j) = \sum_{i=1}^{j} Y(t_i) \tag{10}$$

The series ranges are obtained by obtaining the difference between the maximum value and the minimum value of the accumulated deviations.

$$R(t_j) = \max\Big(Z(t_1), Z(t_2), \ldots, Z(t_j)\Big) - \min\Big(Z(t_1), Z(t_2), \ldots, Z(t_j)\Big) \tag{11}$$

The standard deviation of the series is obtained.

$$S(t_j) = \sqrt{\frac{1}{j}\sum_{i=1}^{j}(X(t_i) - m(t_j))^2} \tag{12}$$

Finally, the rescaled range is calculated as follows

$$(R/S)(t_j) = \frac{R(t_j)}{S(t_j)} \tag{13}$$

It is noted that $(R/S)$ is a dimensionless variable. For a self-similar process, the rescaled rank series satisfies the power law function:

$$(R/S)(t_j) = Kt_j^H \tag{14}$$

$t_j$ corresponds to the scale, $K$ is a constant and $H$ is the Hurst exponent which is estimated as the slope of a log-log plot of $R/S$ versus $t_j$. The asymptotic behavior of the correlation function at infinity determines the presence or absence of long-range dependence. For sufficiently large time series, $H = 0.5$ indicates randomness, $H > 0.5$ implies that a series is persistent which characterizes long-range correlated processes embedded in the series. In contrast, $H < 0.5$ autocorrelation is anti-persistent (Gneiting, & Schlather, 2004).

## 3 Materials and methods

### 3.1 *Flow selection*

In this work, the two-phase downward flow data described by Moguel *et al*. (2021) were used. The physical setup is described from a voltage-time series representing the liquid-gas fraction in a pipe cross section. The device interprets this fraction as a voltage signal, with an acquisition frequency of 1000 Hz, through a PC equipped with a multifunction I/O card and a LabVIEW program. Voltage signals are useful for characterizing biphasic flow patterns as they directly reflect phase retention (Soedarmo *et al*., 2018).

Table 1. Description of flow characteristics (Moguel *et al.*, 2021).

| Flow pattern | SW | | FF | | WA | | LS | |
|---|---|---|---|---|---|---|---|---|
| | A | a | B | b | C | c | D | d |
| $V_{SL}$ (m/s) | 0.5 | 0.5 | 0.05 | 0.05 | 0.7 | 0.7 | 0.7 | 0.7 |
| $V_{SG}$ (m/s) | 0.5 | 0.7 | 0.5 | 0.5 | 3 | 4 | 0.5 | 1 |
| $\theta$ | -45 | -45 | -85 | -80 | -70 | -70 | -70 | -70 |

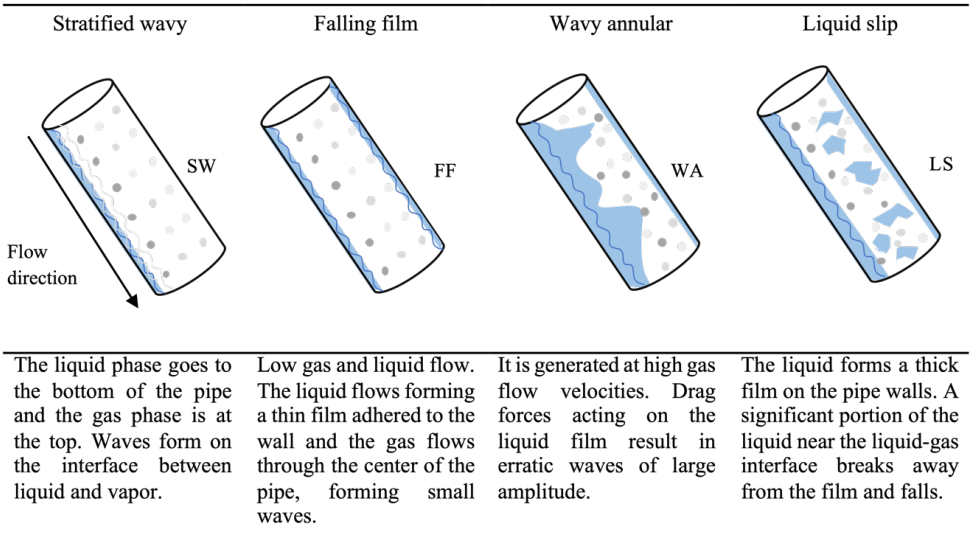


Figure 1. Flow patterns: stratified wavy (SW), falling film (FF), wavy annular flow (WA) and liquid slip flow (LS).

In addition, the series can be easily obtained and reflect an apparently random behavior, interesting characteristics that motivate the proposed analysis.

The complexity of the series has been extensively studied in various areas of science as previously mentioned. However, in the area of chemical engineering, few studies of the complexity in chemical processes have been visualized. Due to the need to have reliable data to validate the proposed analysis, the time series obtained by Moguel *et al.* (2021) of four different flow patterns from an experimental setup. Figure 1 presents the description of these flow patterns; stratified wavy flow (SW) and three subclassifications of annular flow named falling film (FF), wavy annular (WA) and liquid slip (LS). Previously these patterns were characterized according to their wave structure and topology using a high-speed camera (Al-Ruhaimani *et al.*, 2017; Moguel *et al.*, 2021).

### *3.2 Gas-liquid fraction as a voltage time series*

The two-wire capacitance sensor is an electronic device installed in the test section of the pipe. A pair of parallel filaments pass through the cross section of the pipe. The conductivity changes as a function of the amount of liquid, the voltage between the filaments is an instantaneous measurement of the gas-liquid fraction. The voltage response range is 0 to 5 V; the greater the amount of liquid, the higher the voltage. The capacitance sensor is calibrated daily due to weather conditions. In addition, the voltage-time series are normalized for comparison purposes. This normalization is based on the sensor response when the pipe is empty ($V_{min}$) and when it is full ($V_{max}$). If $V$ is a voltage-time series, the normalized signal is $V_0 = (V - V_{min})/(V_{max} - V_{min})$. Voltage measurements were sampled at 1000 Hz for 1 minute, obtaining time series of 60,000 data for each experimental flow pattern. The voltage time series correspond to different gas and liquid velocities, as well as different pipe inclination angles. The time series show an apparently random behavior, with different amplitude ranges.

## 4 Results and discussion

A study of the complexity of the flow patterns for each time series of the flows described in section 4 was performed using the entropy obtained by singular value decomposition and Hurst analysis.

### *4.1 SVD Entropy*

Figure 1 shows the entropy variation for the time series corresponding to the flows: A) stratified wavy (SW); B) falling film (FF); C) wavy annular (WA) and D) liquid slip (LS). For the SW flow the entropy variation with respect to scale exhibits the existence of small fluctuations, using a low pass filter it is observed that

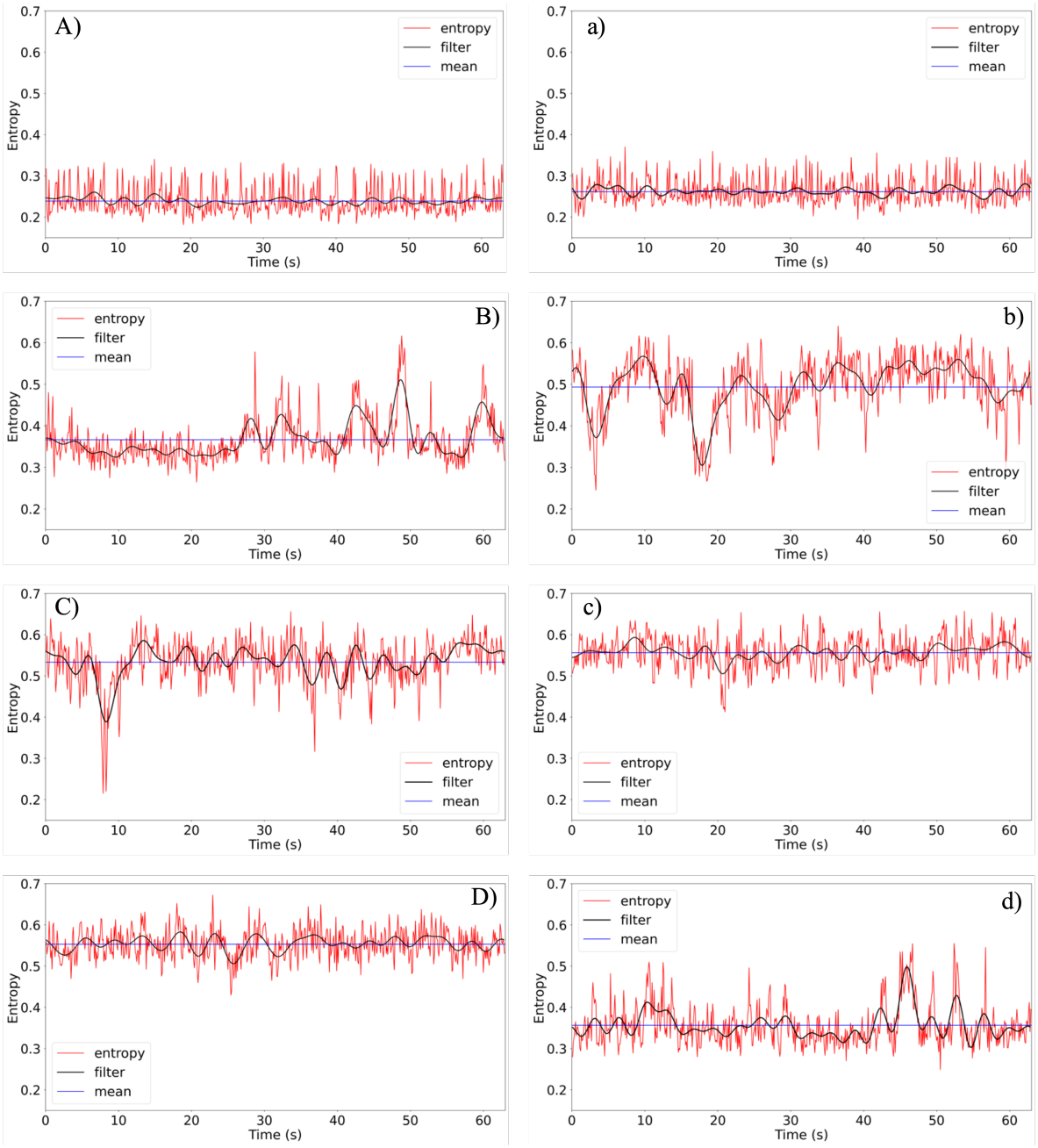


Figure 2. Entropy of four flow patterns: A) SW: $V_{SL}$ = 0.5, $V_{SG}$ = 0.5, angle = -45°; B) FF: $V_{SL}$ = 0.05, $V_{SG}$ = 0.5, angle = -85°; C) WA: $V_{SL}$ = 0.7, $V_{SG}$ = 3, angle = -70°; D) LS: $V_{SL}$ = 0.7, $V_{SG}$ = 0.5, angle = -70°; a) SW: $V_{SL}$ = 0.5, $V_{SG}$ = 0.7, angle = -45°; b) FF: $V_{SL}$ = 0.05, $V_{SG}$ = 0.5, angle = -80°; c) WA: $V_{SL}$ = 0.7, $V_{SG}$ = 4, angle = -70° and d) LS: $V_{SL}$ = 0.7, $V_{SG}$ = 1, angle = -70°.

these fluctuations generate an average entropy of 0.24 approximately. Figure a) corresponding to the SW flow shows an increase in the mean entropy caused by a 0.2 m/s increase in the gas surface velocity. The FF flow pattern exhibits a considerable increase in entropy fluctuations, indicating that the falling film flow pattern is more complex than the stratified wavy one. These fluctuations generate an average entropy of 0.37. On the other hand, Figure b) indicates that a variation produced by the reduction of the inclination angle (reduction of 5 degrees) reflects an increase in entropy, i.e., it is a more complex flow pattern, obtaining an average entropy of 0.49.

Figure C) which corresponds to the WA flow pattern generates a higher entropy compared to the flow patterns of the previous cases with a mean entropy of 0.53. Figure c) indicates that a increase in gas surface velocity generates a increase in mean entropy (0.56), which means a more complex flow pattern. Finally, Figure D) represents the LS flow pattern that generated a behavior with sustained fluctuations with a mean entropy of 0.55. Figure d)

indicates that a doubling of the gas surface velocity results in a decrease of the mean entropy. This may indicate that by increasing the gas surface velocity the entropy behavior increases until it reaches a maximum and then decreases when the gas velocity limit for that flow pattern is exceeded.

Table 2. Average entropy obtained for each flow pattern analyzed.

| Flow pattern | SW | | FF | | WA | | LS | |
|---|---|---|---|---|---|---|---|---|
| | A | a | B | b | C | c | D | d |
| $S_{av}$ | 0.24 | 0.26 | 0.37 | 0.49 | 0.53 | 0.56 | 0.55 | 0.35 |

Table 3. Hurst analysis results obtained for the analyzed flow patterns

| Flow pattern | SW | | FF | | WA | | LS | |
|---|---|---|---|---|---|---|---|---|
| | A | a | B | b | C | c | D | d |
| H | 0.475 | 0.403 | 0.601 | 0.863 | 0.655 | 0.729 | 0.839 | 0.812 |
| K | 14.385 | 49.42 | 6.797 | 1.4 | 7.312 | 1.671 | 1.039 | 1.024 |
| $R^2$ | 0.823 | 0.535 | 0.916 | 0.887 | 0.575 | 0.831 | 0.974 | 0.954 |

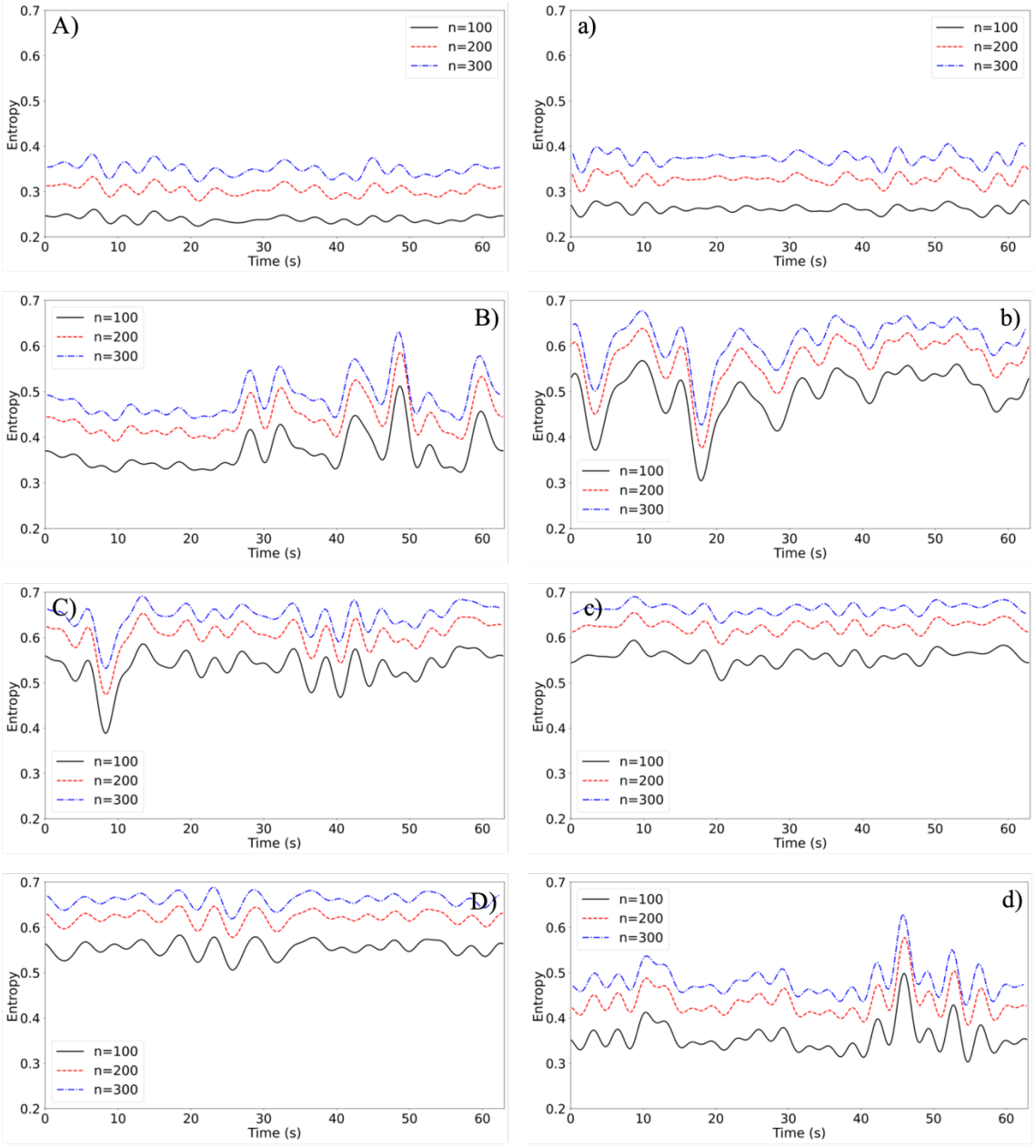

Figure 3. Entropy for different scales for four flow patterns: A) SW: $V_{SL}$ = 0.5, $V_{SG}$ = 0.5, angle = -45°; B) FF: $V_{SL}$ = 0.05, $V_{SG}$ = 0.5, angle = -85°; C) WA: $V_{SL}$ = 0.7, $V_{SG}$ = 3, angle = -70°; D) LS: $V_{SL}$ = 0.7, $V_{SG}$ = 0.5, angle = -70°; a) SW: $V_{SL}$ = 0.5, $V_{SG}$ = 0.7, angle = -45°; b) FF: $V_{SL}$ = 0.05, $V_{SG}$ = 0.5, angle = -80°; c) WA: $V_{SL}$ = 0.7, $V_{SG}$ = 4, angle = -70° and d) LS: $V_{SL}$ = 0.7, $V_{SG}$ = 1, angle = -70°.

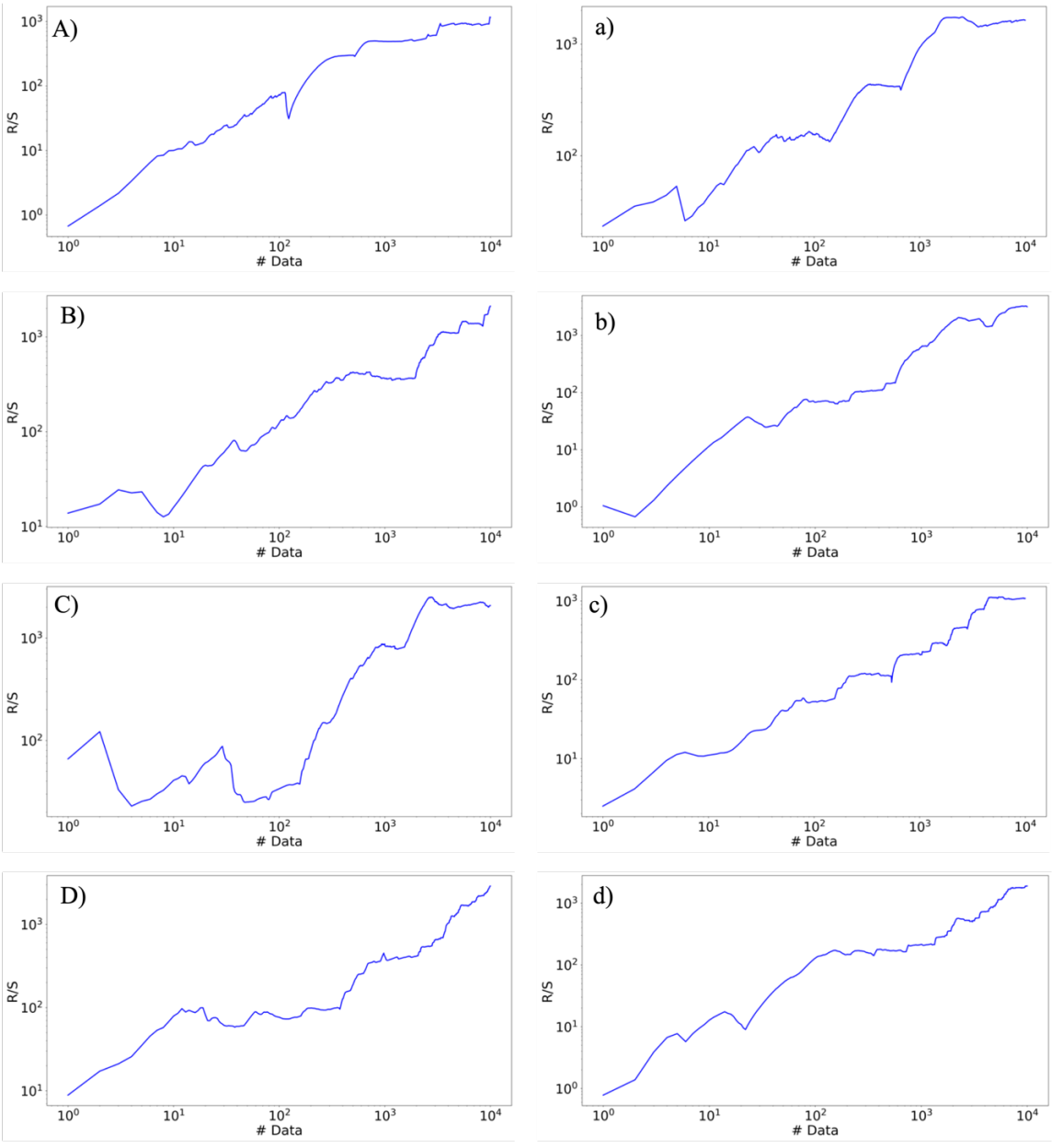


Figure 4. Hurst analysis for four flow patterns: A) SW: $V_{SL}$ = 0.5, $V_{SG}$ = 0.5, angle = -45°; B) FF: $V_{SL}$ = 0.05, $V_{SG}$ = 0.5, angle = -85°; C) WA: $V_{SL}$ = 0.7, $V_{SG}$ = 3, angle = -70°; D) LS: $V_{SL}$ = 0.7, $V_{SG}$ = 0.5, angle = -70°; a) SW: $V_{SL}$ = 0.5, $V_{SG}$ = 0.7, angle = -45°; b) FF: $V_{SL}$ = 0.05, $V_{SG}$ = 0.5, angle = -80°; c) WA: $V_{SL}$ = 0.7, $V_{SG}$ = 4, angle = -70° and d) LS: $V_{SL}$ = 0.7, $V_{SG}$ = 1, angle = -70°.

Table 2 shows the average entropy obtained for each flow pattern analyzed, we can highlight that; a) an increase in the surface velocity of the gas translates into an increase in entropy, this up to a limit value where the flow pattern can be modified, that is, it is altered by the distribution of the gas molecules on the liquid. Subsequently, the entropy decreases when exceeding the maximum limit of gas velocity, this decrease in entropy may be due to the creation of a more orderly flow, by increasing the speed of the gas molecules these pass with such speed so that the time necessary to achieve a total dispersion of gas bubbles is not given, b) the average entropy increases as the gas velocity increases, this result suggests that the gas flow velocity plays an important role in the liquid-gas interaction and c) the decrease of the pipe inclination

angle increases the entropy, which results in a flow pattern with more complexity.

An analysis corresponding to the number of time series data of the study flow patterns showed that the entropy varies with time. This suggests that the stress time series should relate to interactions of phenomena at different time scales associated with the nature of the flow patterns. Therefore, it is convenient to consider the scale-dependent entropy, i.e., with the number of data. Figure 3 presents the variation of entropy with scale, three scales 100, 200 and 300 data were analyzed for the four flow patterns. Figure 3 indicated that the entropy increases with scale, this increase in entropy indicates that; as more data is incorporated, the liquid and gas interaction become more complex for longer time horizons.

### *4.2 Hurts exponent and Rescaled range analysis (R/S)*

Figure 4 shows the rescaled range (R/S) performed on each time series of the four selected flow patterns. From this analysis the Hurst exponent of the SW flow pattern is less than 0.5, which implies an anti-persistent signal. In addition, the other flow patterns studied have Hurst exponents greater than 0.5, indicating the existence of hidden long-range correlations in the time series.

Table 3 presents the condensed results of the global R/S analysis performed on the analyzed flow pattern series. In the SW flow pattern, the Hurst exponent values are less than 0.5 indicating anti-persistent correlations. For the FF, WA and LS flow the Hurts exponent values are greater than 0.5 indicating that the series are persistent. These results suggest that the Hurst exponent can be used as an indicator of changes in the flow regime, as Franca *et al*., (1991) obtained a Hurts exponent of 0.73 for wavy flow patterns which is similar to the results obtained in the present work.

## Conclusions

The use of SVD entropy was explored to study the complexity of liquid-gas two-phase flow patterns. The exact decomposition of the delayed signal matrix in terms of the singular components was performed, and it was determined that the SVD entropy can be easily extended to analyze the complexity of flow patterns at various scales. Also, rescaled analysis indicates that correlations between different flow patterns and the Hurst exponent can be established. The results show correlations associated with the shape characteristics of each type of two-phase flow pattern, which allows characterizing the nonlinear dynamics by R/S analysis. The analysis was able to detect variations of the Hurst exponent as a function of changes in surface velocities, which can be very useful to detect transition phenomena between flow patterns. Therefore, SVD entropy and R/S analysis can complement existing flow pattern identification techniques with the advantage of being easy to apply, having a low computational cost and making use of a single voltage time series.

## References

Aguilar, A., Riesco, J., Pérez, V., Ramírez, J., Rodríguez, J., & Ramírez, A. (2014). Patrones en dos fases para tuberías verticales. *Cuerpos Académicos*, 46.

Al-Ruhaimani, F., Pereyra, E., Sarica, C., Al-Safran, E. M., & Torres, C. F. (2017). Experimental analysis and model evaluation of high-liquid-viscosity two-phase upward vertical pipe flow. *SPE Journal 22*(03), 712-735.

Alvarez-Ramirez, J., Alvarez, J., Rodriguez, E., & Fernandez-Anaya, G. (2008). Time-varying Hurst exponent for US stock markets. *Physica A: Statistical Mechanics and its Applications 387*(24), 6159-6169.

Alvarez-Ramirez, J., Alvarez, J., & Rodriguez, E. (2008). Short-term predictability of crude oil markets: a detrended fluctuation analysis approach. *Energy Economics 30*(5), 2645-2656.

Alvarez-Ramirez, J., Cisneros, M., Ibarra-Valdez, C., & Soriano, A. (2002). Multifractal Hurst analysis of crude oil prices. *Physica A: Statistical Mechanics and its Applications 313*(3-4), 651-670.

Alvarez-Ramirez, J., & Rodriguez, E. (2021). A singular value decomposition entropy approach for testing stock market efficiency. *Physica A: Statistical Mechanics and its Applications 583*, 126337.

Caraiani, P. (2014). The predictive power of singular value decomposition entropy for stock market dynamics. *Physica A: Statistical Mechanics and its Applications 393*, 571-578.

C. Kleinstreuer, P. Griffith. *Two-Phase Flow: Theory and Applications*. Taylor and Francis, New York, NY 2004.

Cheng, L., Ribatski, G., & Thome, J. R. (2008). Two-phase flow patterns and flow-pattern maps: fundamentals and applications. *Applied Mechanics Reviews 61*(5).

Franca, F., Acikgoz, M., Lahey Jr, R. T., & Clausse, A. (1991). The use of fractal techniques for flow regime identification. *International Journal of Multiphase Flow 17*(4), 545-552.

Firouzi, M., & Hashemabadi, S. H. (2009). Exact solution of two-phase stratified flow through the pipes for non-Newtonian Herschel-Bulkley fluids. *International Communications in Heat and Mass Transfer 36*(7), 768-775.

Gneiting, T., & Schlather, M. (2004). Stochastic models that separate fractal dimension and the Hurst effect. *SIAM Review 46*(2), 269-282.

Hewitt, G. F. (1982). *Handbook of Multiphase Systems*. Hemisphere, Washington, DC.

Hurst, H. E. (1951). Long-term storage capacity of reservoirs. *Transactions of the American Society of Civil Engineers 116*(1), 770-799.

Mandelbrot, B. T. (1965). Une classe de processus stochastiques homothetiques a soi-application a la loi climatologique de he Hurst. *Comptes Rendus Hebdomadaires des Seances de l'Academie des Sciences 260*(12), 3274-3277.

Mandelbrot, B. T., Van Ness J. W. (1968). Fractional Brownian motions, fractional noises and applications. *SIAM Rev. 10*, 422-437.

Meraz, M., Rodriguez, E., Femat, R., Echeverria, J. C., & Alvarez-Ramirez, J. (2015). Statistical persistence of air pollutants (O3, SO2, NO2 and PM10) in Mexico City. *Physica A: Statistical Mechanics and its Applications 427*, 202-217.

Moguel-Castañeda, J. G., Rocha-Lara, C. E., Ramirez-Castelan, C. E., Soto-Cortes, G., Hernandez-Martinez, E., & Puebla, H. (2021). Two-phase flow-patterns identification in oil/gas pipelines based on fractal analysis. *The Canadian Journal of Chemical Engineering 99*(4), 874-883.

O'Donovan, A., & Grimes, R. (2020). Two-phase flow regime identification through local temperature mapping. *Experimental Thermal and Fluid Science 115*, 110077.

Peles, Y. P., & Haber, S. (2000). A steady state, one dimensional, model for boiling two phase flow in triangular micro-channel. *International Journal of Multiphase Flow 26*(7), 1095-1115.

Rao, M., Chen, Y., Vemuri, B. C., & Wang, F., (2004). Cumulative residual entropy: a new measure of information. *IEEE Transactions on Information Theory 50*(6), 1220-1228.

Soedarmo, A., Soto-Cortes, G., Pereyra, E., Karami, H., & Sarica, C. (2018). Analogous behavior of pseudo-slug and churn flows in high viscosity liquid system and upward inclined pipes. *International Journal of Multiphase Flow 103*, 61-77.

Sabatini, A. M. (2000). Analysis of postural sway using entropy measures of signal complexity. *Medical and Biological Engineering and Computing 38*(6), 617-624.

Stanley, H. E., Amaral, L. N., Goldberger, A. L., Havlin, S., Ivanov, P. C., & Peng, C. K. (1999). Statistical physics and physiology: monofractal and multifractal approaches. *Physica A: Statistical Mechanics and its Applications 270*(1-2), 309-324.

S. Z. Rouhani, M. S. Sohal, Prog. Nucl. Energy 1983, 11, 219.

Serizawa, A., Feng, Z., & Kawara, Z. (2002). Two-phase flow in microchannels. *Experimental Thermal and Fluid Science 26*(6-7), 703-714.

Wall, M. E., Rechtsteiner, A., & amp; Rocha, L. M., (2003). Singular value decomposition and principal component analysis. *A Practical Approach to Microarray Data Analysis*, 91-109. Springer, Boston, MA.

Wang, Z. (1984). Fast algorithms for the discrete W transform and for the discrete Fourier transform. *IEEE Transactions on Acoustics, Speech, and Signal Processing 4*, 803-816.

Wu, B., Firouzi, M., Mitchell, T., Rufford, T. E., Leonardi, C., & Towler, B. (2017). A critical review of flow maps for gas-liquid flows in vertical pipes and annuli. *Chemical Engineering Journal 326*, 350-377.

Xue, Y., Li, H., Li, L., & Chen, T. (2014). A review of studies on the flow patterns of gas-liquid two phases flow in vertical tubes. *International Journal of Microscale and Nanoscale Thermal and Fluid Transport Phenomena 5*(3/4), 179.